



3 4456 0134295 5

ORNL/TM-8555

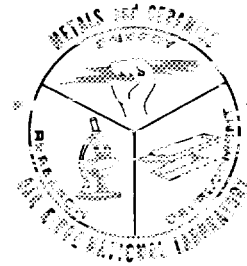
ornl

**OAK
RIDGE
NATIONAL
LABORATORY**



Mechanical Reliability of Current Alumina and Beryllia Ceramics Used in Microwave Windows for Gyrotrons

P. F. Becher
M. K. Ferber



**OPERATED BY
UNION CARBIDE CORPORATION
FOR THE UNITED STATES
DEPARTMENT OF ENERGY**

Printed in the United States of America. Available from:
National Technical Information Service
U.S. Department of Commerce
5285 Port Royal Road, Springfield, Virginia 22161
NTIS price codes - Printed Copy A03, Microfiche A01

This report was prepared as an account of work sponsored by an agency of the United States Government or whether the United States Government or any agency thereof, not any of their employees, makes any warranty, express or implied, or assumes any legal liability or responsibility for the accuracy, completeness, or usefulness of any information, apparatus, product, or process disclosed, or represents that its use would not infringe privately owned rights. Reference herein to any specific commercial product, process, or service, or to any trade name, trademark, manufacturer, or otherwise, does not necessarily constitute or imply its endorsement, recommendation, or favoring by the United States Government or any agency thereof. The views and opinions of authors expressed herein do not necessarily state or reflect those of the United States Government or any agency thereof.

ORNL/TM-8555
Distribution
Category UC-20c

METALS AND CERAMICS DIVISION

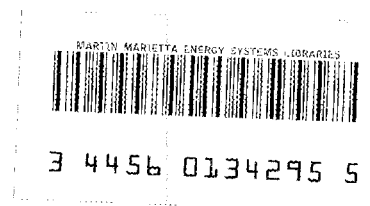
MECHANICAL RELIABILITY OF CURRENT ALUMINA AND BERYLLIA CERAMICS
USED IN MICROWAVE WINDOWS FOR GYROTRONS

P. F. Becher and M. K. Ferber

NOTICE: This document contains information of
a preliminary nature. It is subject to revision
or correction and therefore does not represent
a final report.

Date Published: February 1983

Prepared by the
OAK RIDGE NATIONAL LABORATORY
Oak Ridge, Tennessee 37830
operated by
UNION CARBIDE CORPORATION
for the
Office of Fusion Energy
U.S. Department of Energy
Under Contract No. W-7405-eng-26



CONTENTS

ABSTRACT	1
INTRODUCTION	1
EXPERIMENTAL APPROACH	2
RESULTS AND DISCUSSION	4
INFLUENCE OF SURFACE FINISH	4
DYNAMIC FATIGUE: STRESSING RATE AND ENVIRONMENTAL EFFECTS ON FRACTURE STRENGTHS	5
INERT FRACTURE STRENGTH DISTRIBUTIONS	7
STATIC FATIGUE BEHAVIOR	8
FATIGUE RELIABILITY DIAGRAM	10
SUMMARY	14
ACKNOWLEDGMENTS	15
REFERENCES	15

MECHANICAL RELIABILITY OF CURRENT ALUMINA AND BERYLLIA CERAMICS
USED IN MICROWAVE WINDOWS FOR GYROTRONS

P. F. Becher and M. K. Ferber

ABSTRACT

The mechanical reliability was evaluated for the alumina and beryllia ceramics now used as microwave windows in the high-power (≥ 200 kW) high-frequency (≥ 60 GHz) gyrotron tubes being developed for plasma heating in fusion systems. Analysis of the stresses generated in the various window configurations and tube operating conditions indicated that significant tensile stresses are generated in the ceramic window by dielectric heating. As a result, we characterized the static and dynamic fatigue behavior and the inert strength distributions for these two ceramics (i.e., Wesgo 995 alumina and Thermalox 99 Standard beryllia). The fatigue studies included the behavior in the fluorocarbon fluid used for window cooling at 22 and 48°C and in both air (65% relative humidity) and distilled water at 22°C.

These data were then analyzed in order to construct reliability diagrams for these materials. Such diagrams revealed that the use of these particular grades of these ceramic materials will be limited by their time to failure at the tensile stresses imposed on them in gyrotrons operating at 60 GHz or greater and at least 200 kW in the continuous wave (CW) TE_{02} mode (i.e., radial power distribution in beam exhibits two maxima). Both the fatigue behavior and inert strengths can be improved by the use of ceramics with increased density ($>97\%$ of theoretical) and a uniform fine ($\leq 10 \mu\text{m}$) grain size. Use of these advanced materials would permit significant increases in the mechanical reliability of the gyrotron microwave window.

INTRODUCTION

The mechanical characteristics of two commercial ceramics employed as window materials in microwave heating devices (gyrotrons) were determined and used to describe the potential of these materials for long-term applications. The results of this study will be discussed in the following sequence:

1. flexural fracture strengths — influence of surface finish, inert strength distributions at liquid nitrogen temperatures (i.e., no slow crack growth occurs), and the influence of both the rate of stress application and the environment on strength;
2. static fatigue; and
3. prediction of mechanical reliability.

Steps 1 and 2 constitute the actual experimental sequence followed in deriving the data required for formulating the mechanical reliability. Details on the factors affecting mechanical reliability and on the methodology are published elsewhere.¹ This report describes the long-term mechanical reliability of both a beryllia and an alumina ceramic and demonstrates the significant effects that loading rates and environment have on their measured fracture strength values. These results graphically illustrate the need to know both explicit test conditions represented by the data sets used for design purposes and to have data for a variety of test conditions that simulate the various conditions expected in service.

EXPERIMENTAL APPROACH

The materials examined included samples obtained from a single isostatically pressed and sintered billet of Thermalox 995 standard BeO* and three disks of pressed and sintered AL 995 Al₂O₃.† The BeO ceramic had an average density of 2.904 g/cm³ (96.5% of theoretical), spherical pores (1 to 3 μm in diameter) both within grains and along grain boundaries, and an average grain size of about 35 μm. The Al₂O₃ ceramic had an average density of 3.84 g/cm³ (96.4% of theoretical) with about 2-μm average inter- and intragranular pores distributed in a microstructure consisting of regions of 5- to 8-μm grains in a 30-μm grain size matrix. Typical microstructures for the two materials investigated are illustrated in Fig. 1.

*A product of Brush-Wellman Corp., Elmore, Ohio. Test samples prepared by Ceradyne Corp., Santa Ana, Calif.

†A product of Wesgo, Bellevue, Calif.

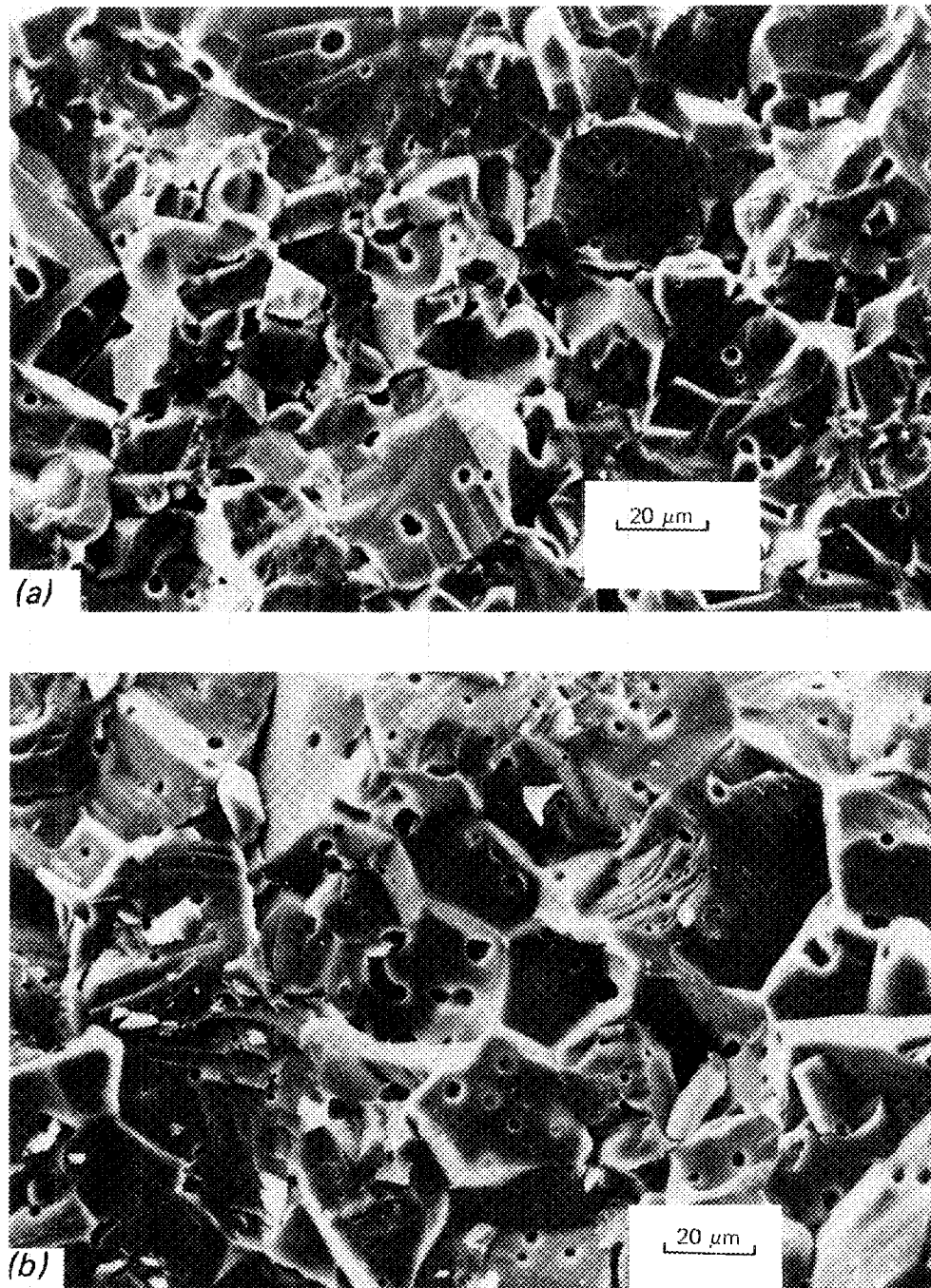


Fig. 1. Fracture surfaces of alumina and beryllia ceramics currently used for microwave windows in gyrotron tubes. (a) A bimodal grain size is evident in the alumina, in which regions containing 5- to 8- μm grains are distributed in a matrix of larger ($\sim 30\text{-}\mu\text{m}$ average) grains. (b) A uniform grain size averaging about 35 μm is observed in the beryllia. Both materials exhibit 1- to 3- μm -diam pores, which are distributed inter- and intragranularly.

Fracture strength and static fatigue data were obtained by employing four-point flexure tests for test span ratios (i.e., of distances between inner and outer load points) of 19.05:31.75 mm and 6.35:19.05 mm. To examine the effects of surface finish on the strength of the beryllia ceramic, a limited number of fracture strength tests were conducted with a three-point flexure fixture having a load span of 38.1 mm. The flexure test bars had cross-sectional dimensions of 2.54 by 2.79 mm and with edges chamfered at 45° (chamfer -0.06 mm in width). The tensile surfaces consisted of 500-grit diamond-ground surfaces for the BeO specimens and either as-fired or 180-grit diamond-ground surfaces for the Al₂O₃ specimens. Except when the effects of the type of surface finish were evaluated, mechanical properties were determined with BeO bars diamond ground in a direction parallel to the tensile axis and with Al₂O₃ bars that had as-fired tensile surfaces. Test environments included liquid nitrogen, air (22°C, 65%–70% relative humidity), water (22°C), and FC-75 fluorocarbon fluid* (22°C) for fracture strengths and FC-75 fluid held at both 22 and 48°C for static fatigue tests. The solubility limit for water of about 7 ppm in the fluorocarbon fluid was confirmed analytically.

RESULTS AND DISCUSSION

The fracture strengths of ceramics are influenced by surface finish, environment, and loading rates as well as by stress state (i.e., uniaxial versus biaxial). Because the important effects of these factors vary for different ceramic materials, we determined their effects on the strengths of the beryllia and alumina ceramics used to fabricate gyrotron tube windows. The results of surface and test conditions on the fracture strengths are presented in the following sections of this report.

INFLUENCE OF SURFACE FINISH

The fracture strengths in three-point flexure for the beryllia ceramic were not significantly influenced by the direction of surface grinding, as shown in Table 1. However, the fracture strengths of as-fired alumina ceramic were slightly increased by surface grinding (Table 1).

*A product of 3M Corp., St. Paul, Minn.

Table 1. Influence of various surface conditions on the flexure strength of polycrystalline alumina and beryllia

Material	Flexure strength (MPa)
<i>Alumina</i>	
As-fired surface	251 ± 12
Surface ground in direction parallel to tensile axis	282 ± 12
<i>Beryllia</i>	
Surface ground in direction parallel to tensile axis	174 ± 12
Surface ground in direction perpendicular to tensile axis	178 ± 8

DYNAMIC FATIGUE: STRESSING RATE AND ENVIRONMENTAL EFFECTS ON FRACTURE STRENGTHS

Except for the data obtained for specimens immersed in liquid nitrogen, the influence of decreasing the rate of application of stress in four-point flexure tests of the alumina ceramic with as-fired tensile surfaces is quite dramatic (Fig. 2). Similar effects are obtained with the beryllia ceramic (Fig. 3). In addition, both figures show that changes in test environment dramatically alter the fracture strengths of these materials. The dynamic fatigue data were fitted by linear regression analysis to the standard expression

$$\ln \sigma_f = \frac{1}{n+1} \ln \dot{\sigma} + A, \quad (1)$$

where σ_f is the fracture strength, $\dot{\sigma}$ is the stressing rate applied, n is the stress corrosion susceptibility factor, and A is a constant. Small values of n , of course, reflect greater susceptibility to slow crack growth and hence more rapid degradation of strength with time under load.

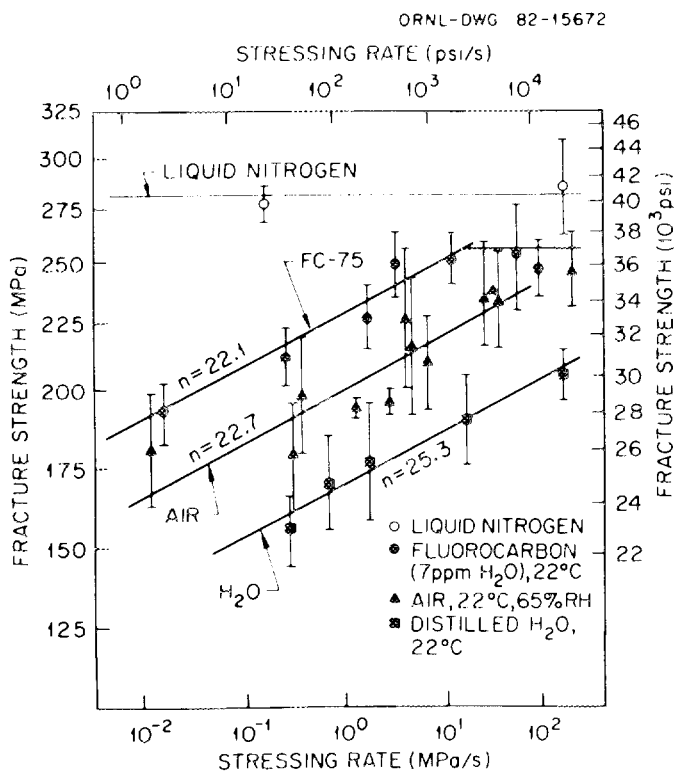


Fig. 2. Dynamic fatigue behavior of polycrystalline alumina. Four-point flexure strength at 22°C illustrates dependence on both environment and stressing rate, indicative of slow crack growth. Such crack growth occurs even in the fluorocarbon fluid used as a window coolant in the gyrotron tube.

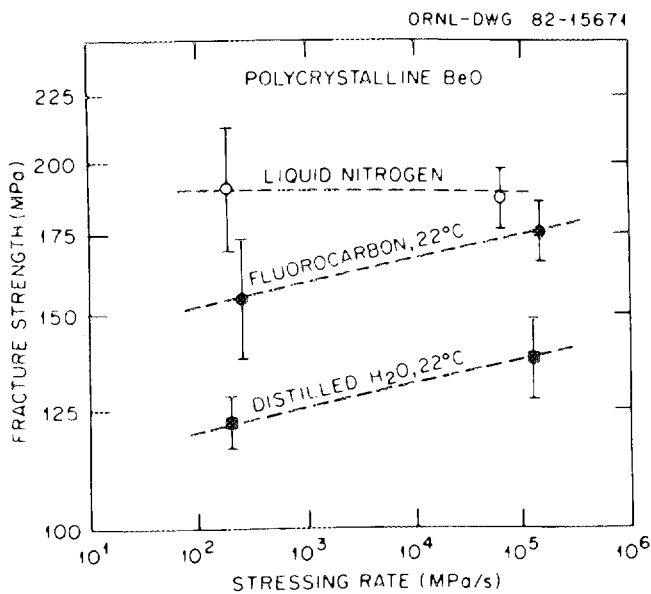


Fig. 3. Dynamic fatigue is indicated by loss of strength of BeO at 22°C with decrease in stressing rate and increase in water content at crack tip.

INERT FRACTURE STRENGTH DISTRIBUTIONS

To obtain the statistical parameters required to describe the variability of fracture strength of these brittle materials due solely to the variability of critical flaw-size populations, flexure strengths were measured in a liquid nitrogen bath to avoid slow crack growth effects during loading. The results of these tests are shown in Fig. 4 as a plot that describes the probability that a specimen will fail when a known stress is applied. The data points, which represent the distribution of strengths obtained in four-point flexure, are then fitted by a linear regression analysis to

$$\ln \ln 1/(1 - P_f) = m \ln(\sigma_{IC}/\sigma_0) , \quad (2)$$

where P_f is the probability of failure, m is the Weibull modulus reflecting the breadth of the flaw size range, σ_{IC} is the inert strength, and σ_0 is a constant. A large value of m reflects a very narrow flaw size range and thus a minimal variability in strength.

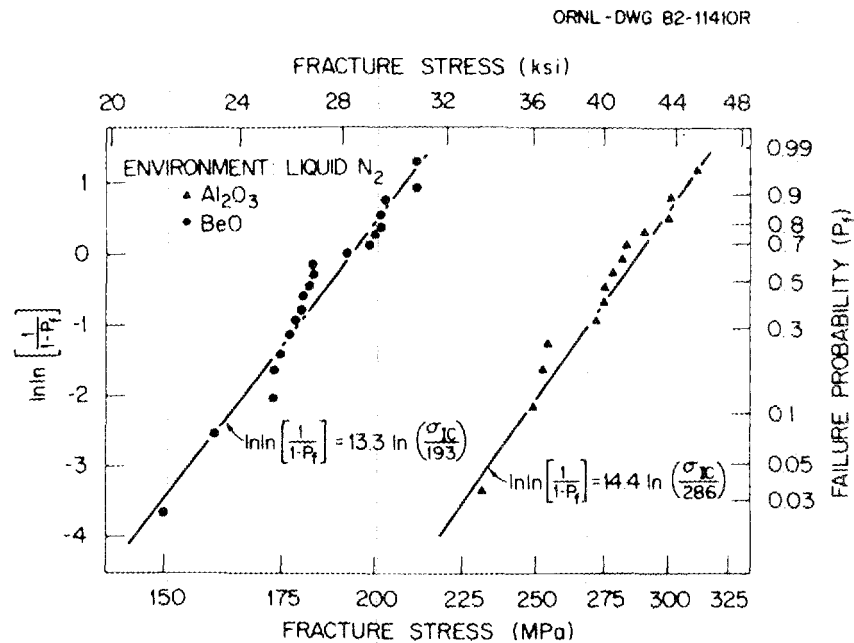


Fig. 4. Distribution of four-point flexure strength under conditions in which slow crack growth is eliminated. This distribution shows the effect of the statistical nature of critical flaw parameters.

STATIC FATIGUE BEHAVIOR

Static fatigue tests were conducted in four-point flexure in a bath containing the fluorocarbon fluid maintained at 22 or 48°C. The time required for the flexure bar to fail upon application of a known stress level is then used to construct the fatigue plots (Fig. 5). The data at 22°C for the Al_2O_3 ceramic exhibit considerably more scatter than do the BeO data (Fig. 5), which undoubtedly reflect the less uniform bimodal microstructure of the Al_2O_3 ceramic.

The BeO data at 22°C give the first firm evidence of a fatigue limit in a polycrystalline ceramic. At applied stresses of less than 40% of the mean inert strength of the BeO, no fatigue (slow crack growth) occurred in the FC-75 fluorocarbon at 22°C. Keep in mind that this does not reflect the statistical nature of failure, only that the fatigue limit is reached at a probability of failure level of approximately 0.5 (about one out of two samples fail).

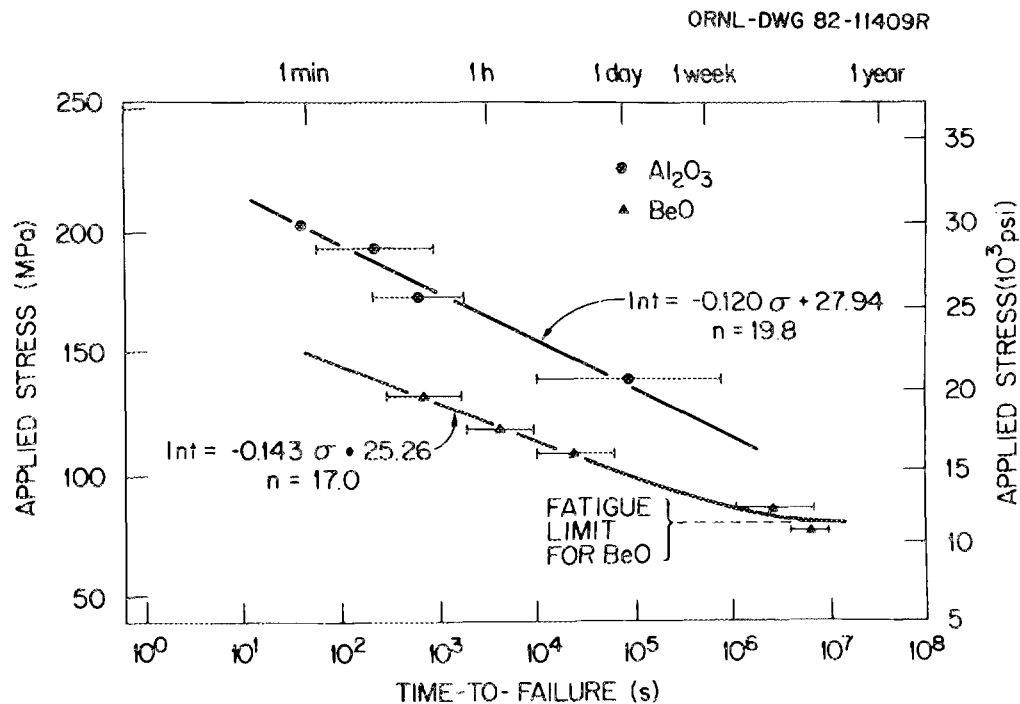


Fig. 5. Static fatigue behavior of ceramics in fluorocarbon fluid (~7 ppm H_2O), showing time to failure dependence on applied flexure stress level at 22°C. Note that the BeO data exhibit a fatigue limit. Both curves represent time to failure for a 0.5 probability of failure.

On the other hand, the fatigue problem is made more severe by increasing the temperature of the fluorocarbon bath. The average time to failure at a given applied stress at 48°C is about one tenth that at 22°C, as seen in Fig. 6.

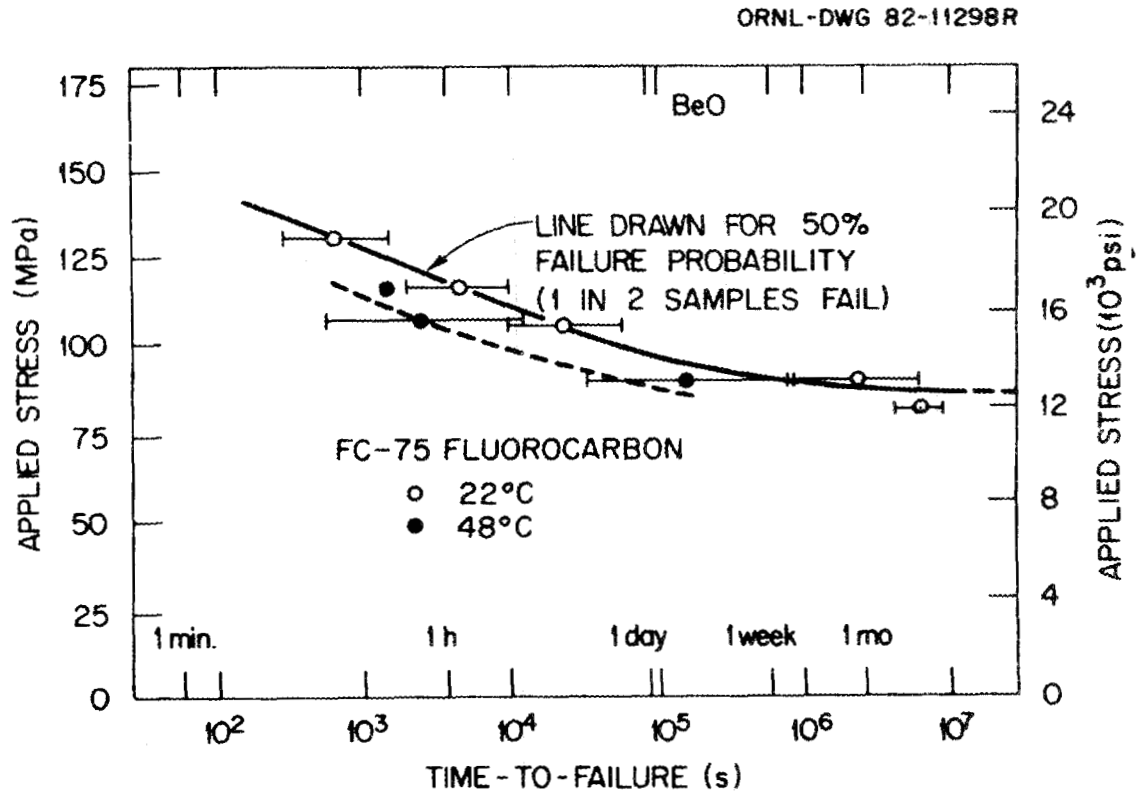


Fig. 6. Increase in temperature increases slow crack growth rates in BeO tested in fluorocarbon fluid. Such increases in temperature could occur in the gyrotron tube as a result of dielectric heating of the ceramic and cooling fluid.

Analysis of the data obtained is possible by linear regression methods except at longer times to failure in the case of BeO, in which nonlinear behavior occurs. This nonlinear region was treated by incorporating a fatigue limit and fitting the data by iterative methods. The linear portions of the time to failure t versus applied stress σ data in Fig. 5 were analyzed by two different approaches. To derive the stress

corrosion susceptibility exponent n and the A parameters used in the life-time prediction, the following was used:

$$\ln t = -n \ln \sigma + A' \quad . \quad (3)$$

A more general form,

$$\ln t = b_1 \sigma + b_0 \quad , \quad (4)$$

can be used to describe the stress corrosion process (e.g., activation volume). The terms b_1 , b_0 , and A' are constants. The n values determined by static fatigue (Fig. 5) and by dynamic fatigue (Fig. 2) are in excellent agreement for the alumina ceramic tested in the fluorocarbon fluid, 19.8 and 22.1, respectively.

The static fatigue limit in the BeO was described by using the general integral representation of fatigue life:

$$t = (2/\sigma^2 Y^2) \int_{\sigma(K_{IC}/\sigma_{IC})}^{K_{IC}} (K_I/V) dK_I \quad , \quad (5)$$

where the crack velocity V is determined by iteration processes by

$$V = \Omega_2 \exp(\Omega_3 K_I) \{1 - \exp[-L(K_I - K^*)]\} \quad , \quad (6)$$

where K_I is a crack tip stress intensity factor and is less than K_{IC} , the critical stress intensity factor; Y is a geometric factor; and Ω_2 , Ω_3 , L , and K^* are constants obtained by iteration; L and K^* characterize the fatigue limit.

FATIGUE RELIABILITY DIAGRAM

When combined with the probability-of-failure data, the measured static fatigue behavior can be used to predict the fatigue behavior for various levels of probability of failure (i.e., $1 -$ probability of survivability). One can recognize that the predictions are influenced by the

number of data points in the sets (i.e., the confidence limits for each probability level will decrease with increasing number of data points). However, it is extremely useful to observe what happens when desired probability of failure levels are prescribed.

This is accomplished by applying the analysis for the time to failure t at various applied stress σ_a levels,

$$t = \frac{(2K_{IC}/\sigma_0)^{2-n}}{AY^2(n-2)} \sigma_a^{-n} \left(\ln \ln \frac{1}{1 - P_f} \right)^{(n-2)/m}, \quad (7)$$

where the values of the required parameters (Table 2) are obtained from the experimental data in Figs. 4 and 5 except for the values of the critical stress intensity factor K_{IC} , which were obtained from the applied-moment double-cantilever test specimens.

Table 2. Fracture mechanics parameters derived for the window materials

Parameter	995S BeO	AL 995 Al ₂ O ₃
K_{IC} , MPa·m ^{1/2}	4.8	4.5
n	17	19.8
A'	1.07×10^{-11}	7.34×10^{-13}
Y	$\sqrt{\pi}$	$\sqrt{\pi}$
m	13.3	14.4
σ_0 , MPa	193	286

The resultant design diagrams for the Thermalox 995 standard BeO and the AL 995 alumina are shown in Figs. 7 and 8, respectively. Incorporated into each diagram are estimated levels of the tensile stress generated in a window of a CW gyrotron tube operating at 60 GHz in the TE₀₂ mode at a 200-kW power level.^{2,3}

Use of the fatigue data for the flexure bars with the calculated service stress levels in a window disk will yield a somewhat greater

ORNL-DWG 82-11408

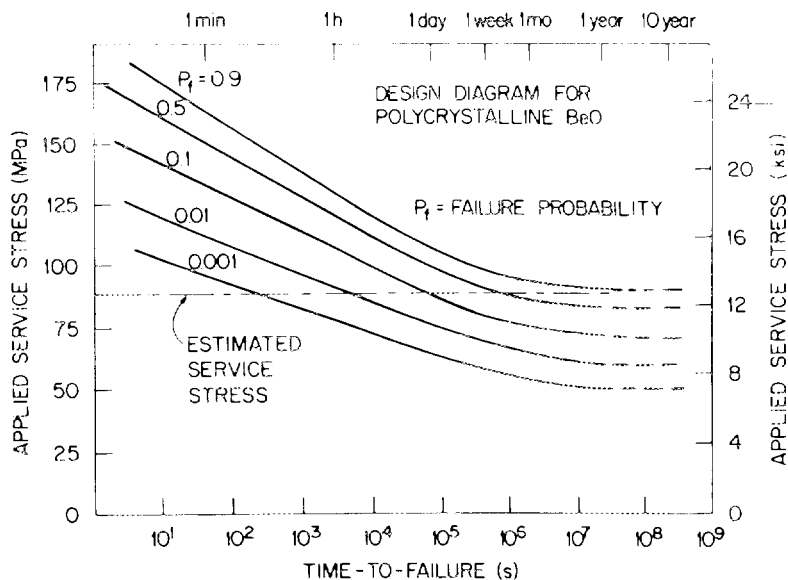


Fig. 7. Design diagram for BeO ceramic represents time to failure versus applied flexure stress level for various probability of failure levels at 22°C. The service stress level was determined by analysis of radial and axial tensile stresses generated in a double-disk window structure (each disk being about 76 mm in diameter and 2.5 mm thick), in which fluorocarbon coolant passes between the two parallel disks. The gyrotron operating conditions consisted of 200 kW of power at 60 GHz.

ORNL-DWG 82-11829

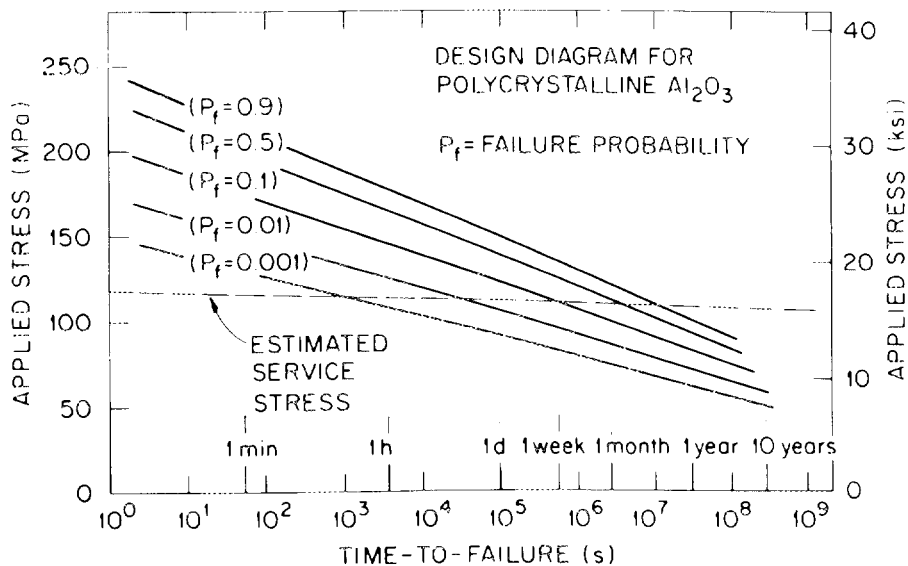


Fig. 8. Design diagram for alumina ceramic based on static fatigue behavior at 22°C. Service tensile stresses analyzed for conditions comparable to those used for BeO windows.

reliability for the design life of a window disk. This is related to two factors. First, the service stresses have been calculated in a manner requiring that the energy level and energy density remain constant with no spurious increases in local energy density as might occur in actual tube operation. Second, the fatigue data are based on samples having both smaller surface area and volume than the actual window. Because both the strength distributions and the time to failure increase with decreasing surface area or volume, the reliability diagrams will predict slightly longer time to failures (at each chosen probability of failure level) than may occur in an actual window.

For either material, the design diagrams indicate that about one of two windows will fail in approximately one month under such calculated service stresses at a temperature of 22°C. On the other hand, if only 1 in 1000 windows can fail, then the service lifetime would be less than 1 h. Obviously, neither of these results is satisfactory if long lifetimes and high survivability are desired for the window. In addition, the present results, which show decreasing fatigue life with increasing temperature of the fluorocarbon fluid (Fig. 6), point out that the above predicted lifetimes will decrease with any increase in the temperature at the ceramic-coolant interface due to microwave heating.

These materials are, however, adequate for short-term testing during the development of 60-GHz tubes, although reliable long-term tube operation may not be achieved with such materials.

One therefore needs to look for materials improvements that can be achieved in the near term. Recent findings on the fatigue behavior of anisotropic noncubic polycrystalline alumina indicate that greater fatigue resistance can be obtained by reducing the grain size.⁴ It is also well known that the critical fracture strength of polycrystalline ceramics can be increased by increasing their density or reducing their grain size. Thus, substantial improvements in the mechanical reliability of the window can be obtained by additional refinements in processing the materials to achieve both densities greater than 97% of theoretical and

uniform grain sizes of less than 10 μm . In fact, a small effort in progress has shown that BeO ceramics having densities greater than 99% of theoretical and grain sizes of less than 5 μm can readily be achieved by hot-pressing fine (submicron) BeO powders obtained by ball milling and the use of less than 4 wt % MgO additions.⁵ Studies are under way to determine the mechanical reliability of windows made from such improved materials.

SUMMARY

1. The mechanical properties pertinent to the gyrotron window reliability of both the Thermalox 995 standard BeO and the AL 995 Al₂O₃ ceramics have been determined. These properties include the critical (inert) fracture strength distribution, static fatigue behavior in the liquid fluorocarbon environment used as a window coolant at 22 and 48°C, and dynamic fatigue in air and water at 22°C.

2. These results show that environmentally assisted slow crack growth (fatigue) occurs in both of the polycrystalline ceramics in the fluorocarbon fluid, which contains only 7 ppm H₂O (the solubility limit). The fatigue rate is increased nearly tenfold by increasing the test temperature from 22 to 48°C.

3. Design diagrams based on the above data reveal that these materials are probably not satisfactory for long service life and high survivability levels at the estimated service stress levels determined by analysis of microwave heating in the TE₀₂ mode. However, such materials are probably adequate for tube design development and short-term testing except at operating frequencies greater than 60 GHz.

4. In the near term, advanced materials could be obtained by improving the process for BeO and Al₂O₃ ceramics. Materials having densities greater than 97% of theoretical and uniform grain sizes of less than 10 μm offer the potential for significantly improving the mechanical reliability of the gyrotron window.

ACKNOWLEDGMENTS

Both the support of and technical interactions with C. M. Loring of the ORNL Fusion Energy Division have contributed substantially to the progress of this study. The authors acknowledge the contributions by S. B. Waters and L. L. Hall in conducting these experiments and by H. Kimery on the analysis of stresses generated by dielectric heating. Appreciation is expressed to F. E. Stooksbury for manuscript preparation and to D. L. LeComte for final preparation.

REFERENCES

1. P. F. Becher, M. K. Ferber, and V. J. Tennery, *Mechanical Reliability of Ceramics for Microwave Window Applications*, ORNL/TM-7811, July 1981.
2. M. K. Ferber, "Subcritical Crack Propagation in Al_2O_3 and BeO Exposed to Reactive and 'Inert' Environments," *Am. Ceram. Soc. Bull.* 61(3), 415 (1982).
3. M. K. Ferber and H. Kimery, "Analysis of Stresses Generated in Ceramics by Microwave Heating," in preparation.
4. A. J. Gesing and R. C. Bradt, "A Microcracking Model for the Effect of Grain Size on Slow Crack Growth in Polycrystalline Al_2O_3 ," in *Fracture Mechanics of Ceramics*, R. C. Bradt, D. P. H. Hasselman, F. F. Lange, and A. G. Evans, eds., Plenum Press, New York, in publication.
5. T. G. Godfrey, Union Carbide Corp., Oak Ridge Y-12 Plant, private communication (1982).

INTERNAL DISTRIBUTION

- | | | | |
|--------|---|-----|------------------------------|
| 1-2. | Central Research Library | 33. | H. H. Haselton |
| 3. | Document Reference Section | 34. | R. P. Jernigan |
| 4-5. | Laboratory Records Department | 35. | W. J. Lackey |
| 6. | Laboratory Records, ORNL RC | 36. | R. J. Lauf |
| 7. | ORNL Patent Section | 37. | J. Lin |
| 8. | Fusion Energy Division Library | 38. | C. M. Loring |
| 9. | Fusion Energy Division
Communications Center | 39. | R. W. McClung |
| 10. | P. Angelini | 40. | H. C. McCurdy |
| 11-15. | P. F. Becher | 41. | O. B. Morgan, Jr. |
| 16. | A. L. Boch | 42. | R. K. Nanstad |
| 17. | R. A. Bradley | 43. | M. J. Saltmarsh |
| 18. | C. R. Brinkman | 44. | A. C. Schaffhauser |
| 19. | J. L. Burke | 45. | J. L. Scott |
| 20. | A. J. Caputo | 46. | J. Sheffield |
| 21. | G. W. Clark | 47. | J. O. Stiegler |
| 22. | R. J. Colchin | 48. | D. P. Stinton |
| 23-24. | F. R. Cox | 49. | T. L. White |
| 25. | H. O. Eason | 50. | F. W. Wiffen |
| 26. | W. P. Eatherly | 51. | Alan Lawley (Consultant) |
| 27. | O. C. Eldridge | 52. | T. B. Massalski (Consultant) |
| 28-32. | M. K. Ferber | 53. | R. H. Redwine (Consultant) |
| | | 54. | K. M. Zwilsky (Consultant) |

EXTERNAL DISTRIBUTION

55. K. Button, Massachusetts Institute of Technology, Bitter National Magnet Lab., 170 Albany St., Cambridge, MA 02139
56. L. J. Craig, Varian Associates, Inc., 611 Hansen Way, Palo Alto, CA 94303
57. R. A. Dandl, 1122 Calle De Los Serranos, San Marcos, CA 92069
58. R. DeBellis, McDonnell Douglas Astronautics Co., P.O. Box 516, St. Louis, MO 63166
59. J. F. Decker, Office of Fusion Energy, Department of Energy, APP, Rm. 219, ER054, GTN, Washington, DC 20545

60. W. P. Ernst, Princeton University, Plasma Physics Laboratory,
P.O. Box 451, Princeton, NJ 08540
61. S. Evans, Varian Associates, Inc., 611 Hansen Way,
Palo Alto, CA 94303
62. S. W. Freiman, Fracture and Deformation Division, National Bureau
of Standards, Washington, DC 20234
63. W. Friz, AFAL/DHM, Wright Patterson AFB, OH 45433
64. T. V. George, Office of Fusion Energy (ETM), Department of Energy,
ER-531, GTN, Washington, DC 20545
65. T. Godlove, Particle Beam Program, Office of Inertial Fusion,
Department of Energy, Mail Stop C-404, Washington, DC 20545
66. V. L. Granatstein, Naval Research Laboratory, Code 6740,
Washington, DC 20545
67. G. M. Haas, Component Development Branch, Office of
Fusion Energy (ETM), Department of Energy, ER-531, GTN,
Washington, DC 20545
68. M. Haas, Naval Research Laboratory, Code 6510, Washington, DC 20375
69. G. W. Hamilton, Reactor Design, MFE Program, Lawrence Livermore
National Laboratory, L6-44, P.O. Box 5511, Livermore, CA 94550
70. J. L. Hirshfield, Yale University, Department of Engineering and
Applied Science, P.O. Box 2159, Yale Station, New Haven, CT 06520
71. G. Ho, Varian Associates, Inc., 611 Hansen Way, Palo Alto, CA 94303
72. W. Ho, Rockwell International, 1049 Camino Dos Rios,
Thousand Oaks, CA 91360
73. G. Hurley, Los Alamos National Laboratory, MS546,
Los Alamos, NM 87545
74. T. James, Office of Fusion Energy, Department of Energy, ER-522,
GTN, Washington, DC 20545
75. H. Jory, Varian Associates, Inc., 611 Hansen Way, Palo Alto, CA 94303
76. K. Krause, Lawrence Livermore National Laboratory,
P.O. Box 808/L-443, Livermore, CA 94550
77. J. V. Lebacqz, Stanford Linear Accelerator Center, P.O. Box 4349,
Stanford, CA 94305

78. W. Lindquist, Electronics Engineering Department, Lawrence Livermore Laboratory, P.O. Box 808/L-443, Livermore, CA 94550
79. C. Moeller, General Atomic Co., P.O. Box 81608, San Diego, CA 92138
80. K. Moses, JAYCOR, 2811 Wilshire Boulevard, Suite 690, Santa Monica, CA 90403
81. J. Moskowitz, Ceradyne, Inc., 3030-A S. Red Hill Ave., Santa Ana, CA 92705
82. J. H. Pfannmuller, McDonnell Douglas Astronautics Co., c/o Oak Ridge National Laboratory, P.O. Box Y, Bldg. 9983-32, Oak Ridge, TN 37830
83. G. F. Pierce, 53 Lomond Drive, Inverness, IL 60067
84. R. Pohanka, Office of Naval Research, 800 North Quincy Street, Arlington, VA 22217
85. B. H. Quon, TRW Defense and Space Systems, 1 Space Park, Bldg. R-1, Redondo Beach, CA 90278
86. M. E. Read, Naval Research Laboratory, Code 6740, Washington, DC 20375
87. D. B. Remsen, General Atomic Company, P.O. Box 81608, San Diego, CA 92138
88. R. W. Rice, Naval Research Lab., Code 6360, 4555 Overlook Ave., S.W. Washington, DC 20375
89. T. Roemesser, TRW Defense and Safety Space Systems, 1 Space Park, Bldg. R-1, Redondo Beach, CA 90278
90. G. Simonis, Harry Diamond Laboratory, 2800 Powder Mill Road, Adelphi, MD 20783
91. W. S. Smith, Wesgo Dir., GET Products Corp., 477 Harbor Blvd., Belmont, CA 94002
92. M. Sparks, Scientific Research Center, 9507 High Ridge Place, Beverly Hills, CA 90210
93. B. Stallard, Lawrence Livermore Laboratory, University of California, L-437, P.O. Box 808, Livermore, CA 94550
94. H. S. Staten, Office of Fusion Energy (ETM), Department of Energy, ER-531, GTN, Washington, DC 20545

95. P. J. Tallerico, AT-1, Accelerator Technology Division,
Los Alamos Scientific Laboratory, Mail Stop H827, P.O. Box 1663,
Los Alamos, NM 87545
96. J. J. Tancredi, Hughes Aircraft Company, Electron Dynamics
Division, 3100 W. Lomita Blvd., Torrance, CA 90509
97. R. J. Temkin, National Magnet Laboratory, Massachusetts Institute
of Technology, Cambridge, MA 02139
98. Director, U.S. Army Ballistic Missile Defense Advance Technology
Center, Attn.: D. Schenk, ATC-R, P.O. Box 1500,
Huntsville, AL 35807
99. RADC/OCTP, Griffiss AFB, NY 13441
100. Office of Assistant Manager for Energy Research and Development,
Oak Ridge Operations Office, Department of Energy,
Oak Ridge, TN 37830
- 101-284. Department of Energy Technical Information Center,
Oak Ridge, TN 37830

For distribution as shown in TID-4500 Distribution Category
UC-20c (Magnetic Fusion Energy, Reactor Materials)